

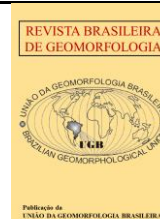


<https://rbgeomorfologia.org.br/>
ISSN 2236-5664

Revista Brasileira de Geomorfologia

v. 26, nº 3 (2025)

<http://dx.doi.org/10.20502/rbg.v26i3.2606>



Research Article

Geomorphological Mapping of the gully erosion in the Brazilian Cerrado using Remotely Piloted Aircraft (RPA)

Mapeamento geomorfológico de voçoroca no Cerrado brasileiro com uso de Aeronave Remotamente Pilotada (RPA)

Willian Toshiaki Mizumura ¹, Alan Silveira ², Juliana Abreu Crosara Petronzio ³, Samuel Lacerda de Andrade ⁴, Valdiney José da Silva ⁵

¹ Universidade Estadual Paulista (UNESP), Departamento de Geografia e Planejamento Ambiental (DPGA), Rio Claro, Brasil. willian.mizumura@unesp.br.
ORCID: <https://orcid.org/0009-0007-9525-4407>

² Universidade Federal de Uberlândia (UFU), Instituto de Geografia, Geociências e Saúde Coletiva (IGESC), Uberlândia, Brasil. alan.silveira@ufu.br.
ORCID: <https://orcid.org/0000-0001-7144-8038>

³ Universidade Federal de Uberlândia (UFU), Instituto de Geografia, Geociências e Saúde Coletiva (IGESC), Monte Carmelo, Brasil. julianapetronzio@ufu.br.
ORCID: <https://orcid.org/0009-0001-0405-1169>

⁴ Universidade Federal de Uberlândia (UFU), Instituto de Geografia, Geociências e Saúde Coletiva (IGESC), Monte Carmelo, Brasil. samuelandrade@ufu.br.
ORCID: <https://orcid.org/0000-0002-8119-0840>

⁵ Universidade Federal de Uberlândia (UFU), Instituto de Geografia, Geociências e Saúde Coletiva (IGESC), Monte Carmelo, Brasil. valdiney@ufu.br.
ORCID: <https://orcid.org/0000-0002-2247-2493>

Received: 12/08/2024; Accepted: 14/07/2025; Published: 12/08/2025

Abstract: Detailed geomorphological mapping employs imagery acquired by Remotely Piloted Aircraft (RPA) to investigate gullies, generating morphometric data. This study aimed to develop a detailed geomorphological map, defining geomorphological compartments and recording discrete landform features both within and around the gully, using traditional and adapted symbology. The study area corresponds to the Mombuca Gully in the Brazilian Cerrado, at Monte Carmelo (Minas Gerais, Brazil). The methodology was divided into pre-field, field, and post-field stages, encompassing flight planning; image acquisition with the DJI (Da-Jiang Innovations) Mavic Pro RPA in three scenarios; image treatment, processing, and photo-interpretation to generate morphometric and geomorphological maps. The study identified five geomorphological compartments and documented denudational features, aggradational features, anthropogenic landforms, technogenic deposits, alterations of original channel courses, and the installation of impoundments. Integrated analysis of these data enabled an understanding of natural erosive dynamics and anthropogenic influences. The results support methodological discussions on geomorphological mapping of gullies using high-resolution imagery.

Keywords: geomorphological cartography; linear erosion; unmanned aerial vehicle.

Resumo: A cartografia geomorfológica de detalhe utiliza imagens obtidas por Aeronaves Remotamente Pilotadas (RPA) na investigação de voçorocas, gerando dados morfométricos. Este trabalho teve como objetivo elaborar um mapeamento geomorfológico de detalhe, com definição de compartimentos e registro de feições individualizadas no interior e no entorno

da voçoroca, empregando simbologias tradicionais e adaptadas. A área de estudo corresponde à voçoroca do Mombuca, no cerrado brasileiro, em Monte Carmelo (Minas Gerais – MG). A metodologia dividiu-se em pré-campo, campo e pós-campo, contemplando planejamento de voo, aquisição de imagens pela Aeronave Remotamente Pilotada (RPA) da DJI (Da-Jiang Innovations), modelo Mavic Pro, em três cenários, tratamento das imagens, processamento e fotointerpretação para geração de mapeamentos morfométricos e geomorfológico. O estudo identificou cinco compartimentos geomorfológicos e registrou feições denudativas, feições agradacionais, modelados antrópicos, depósitos tecnogênicos, alterações de cursos fluviais originais e instalação de represamento. A análise integrada dos dados permitiu compreender a dinâmica erosiva natural e as influências antrópicas. Os resultados apoiam discussões metodológicas sobre mapeamentos geomorfológicos de voçorocas a partir de imagens de alta resolução.

Palavras-chave: cartografia geomorfológica; erosão linear; drone.

1. Introduction

Erosion is an intrinsic theme of geomorphology, as it derives from natural processes that sculpt the relief forms of the Earth's surface on a geological time scale. The phenomenon can be affected and driven by anthropogenic activities, which positions man as an important geomorphological agent (Nir, 1983). Thus, erosion constitutes a natural process that occurs in any system, even in balanced ones, and human intervention can accelerate it (Hernani et al., 2002).

According to Goudie (2004), the main factors that control erosion include lithology, tectonics, climate, vegetation and human actions. Castro and Hernani (2015) emphasize the role of “fragile soils”, a term often used for soils with a sandy surface texture, which are more susceptible to water and/or wind erosion than clayey soils (Albuquerque et al., 2015). Guerra (2011) defines erosion as the process of removal of material by rainwater, which is highly frequent in tropical countries such as Brazil.

Linear erosion features are classified as rills, ravines, and gullies (Stabile; Vieira, 2010). Rills are formed by the removal of materials resulting from the action of pluvial water, creating small channels on the surface (Fournier, 1960). Over time, they can evolve into ravines, which represent a higher erosional stage (Araújo, 2011). Upon reaching the water table, the evolution of ravines can give rise to gullies (Almeida Filho; Teixeira Filho, 2014). Pereira and Rodrigues (2022), in a recent literature review, note that the distinction between ravines and gullies, in national and international scenarios, is often established by dimensional criteria. The authors, however, consider the need to consider the behavior of the water table and the infiltration dynamics. Gullies are linear water erosions that demonstrate the intensity of pluvial processes, resulting in large, deep and wide structures (Guerra, 2010).

Erosive processes cause environmental and socioeconomic problems in rural and urban areas (Pereira, 2020). Such processes result in the loss of nutrients from the upper layers of the soil, reduce root penetration and water retention, restrict areas for agricultural activities and cause the sedimentation of water bodies, among other consequences (Guerra; Jorge, 2017). Examples of these problems were recently reported in the city of Buriticupu (MA), where homes collapsed into the interior of the erosional features due to their expansion (Fróes, 2023; Cardoso, 2024).

Inadequate land use, associated with deforestation, lack of planning, absence of conservation practices and incorrect management, aggravates erosion processes. Such factors increase soil exposure to rainfall and susceptibility to the formation of gullies (Hernani et al. 2002). Frequently, gullies are filled with materials of human origin, such as from construction, waste from borrowed materials, and solid waste, with the mistaken purpose of infilling or containing the advance of erosion. According to França Junior and Peloggia (2020), human action transforms the physiography of the landscape, creating landforms (technogenic relief) from sedimentary deposits related to its own activity (technogenic). Moura et al. (2023) proposed guidelines for the registration and classification of technogenic landforms, considering their areal and linear representativeness according to the cartographic scale adopted in the investigation.

Erosional features, especially linear ones such as gullies, are subject to cartographic representation. This contributes to their interpretation and analysis, in addition to supporting the planning of the occupation and recovery of degraded areas. In this context, the role of geomorphological cartography is evident, especially those dedicated to mapping on a detailed scale, as illustrated by the works of Tricart (1965) and Verstappen and Zuidan (1975), widely used in Brazil for their range of symbologies. In a study on the construction of geomorphological

symbols, Silva, Souza and Lupinacci (2022) report that the use of lines and points constitutes a solution for mapping relief features on a detailed scale, a procedure adopted by classical and contemporary authors. When addressing detailed geomorphological mapping, Simon and Lupinacci (2019) discuss the importance of cartographic detailing for understanding spatial dynamics. Such mapping is fundamental to physical-environmental planning, by allowing the identification and individualization of landforms, agents and related processes, with the subsequent grouping and definition of geomorphological units.

Traditionally, gully analysis and monitoring were performed using stakes to monitor their evolving process (Guerra, 1996). Recently, Remotely Piloted Aircraft (RPA), popularly known as drones, have been used for these analyses and monitoring. The technical bulletin by Figueiredo and Figueiredo (2018) describes the steps for conducting RPA flights and acquiring images in aerial surveys. The study by Moura, Santos and Alves Junior (2021) addresses the processing of RPA aerial photographs and the production of the Digital Surface Model (DSM), Digital Terrain Model (DTM), orthomosaics, and contour lines, focusing on the generation of morphometric data for the study of a gully in Anápolis (GO). Rademan and Trentin (2020) used the generation of morphometric information from RPA images to determine the areas of greatest gully advancement in Cacequi (RS). The investigation by Julian and Nunes (2020) used RPA and geoprocessing to calculate the volume of soil eroded in a gully in Marília (SP).

The use of RPA images in geomorphological studies of gullies has been increasing, especially with a focus on producing morphometric information. However, the creation of detailed geomorphological maps that present the identification and individualization of discrete landforms, grouped into geomorphological units as indicated by Simon and Lupinacci (2019), is not common as a final cartographic product. The cartographic individualization of landforms in gullies occurs, for example, in the study by Stefanuto and Lupinacci (2023), who used RPA images to superimpose individualized geomorphological symbols on erosional features in Corumbataí (SP). In this work, the authors mapped the detailed features in the erosion structure using photointerpretation with line and point symbols.

From this perspective, this work aimed to develop a detailed geomorphological map using RPA images. The mapping included, through photointerpretation, the recording of individualized relief features inside and around the Mombuca gully, including those of human origin, through specific symbologies. Additionally, the same mapping proposed a compartmentalization of the gully, based on morphometric data and photointerpretation. Thus, the present study sought to organize a detailed geomorphological map that would identify the compartments of the gully and their individualized features. To this end, concepts and symbologies of detailed geomorphological cartography were used, in addition to technical resources of remote sensing and geoprocessing for the acquisition and treatment of RPA images.

2. Study Area

The proposed geomorphological mapping is applicable to land use and occupation planning and to the recovery of degraded areas, since the Mombuca gully is located in an area under intense influence of urban anthropogenic actions, particularly due to its filling with technogenic deposits. The feature is located in the vicinity of the city of Monte Carmelo, in the Triângulo Mineiro/Alto Paranaíba Mesoregion, and is approximately 2.5 km from the urban area, with a total area of 0.6 km² (Figure 1).

The anthropogenic context, combined with the presence of fragile soils and saprolites derived from granitoids from the Monte Carmelo complex (Codemig, 2017) in an area of the Brazilian Cerrado, justifies the choice of the site as the object of study. Fieldwork carried out in areas of this granite complex revealed linear erosion processes associated with the fragility of the surface cover. This cover is marked by materials susceptible to physical-hydrological dynamics in tropical climate conditions (Barbosa et al., 2018; Casagrande, 2023; Estrada, 2023).

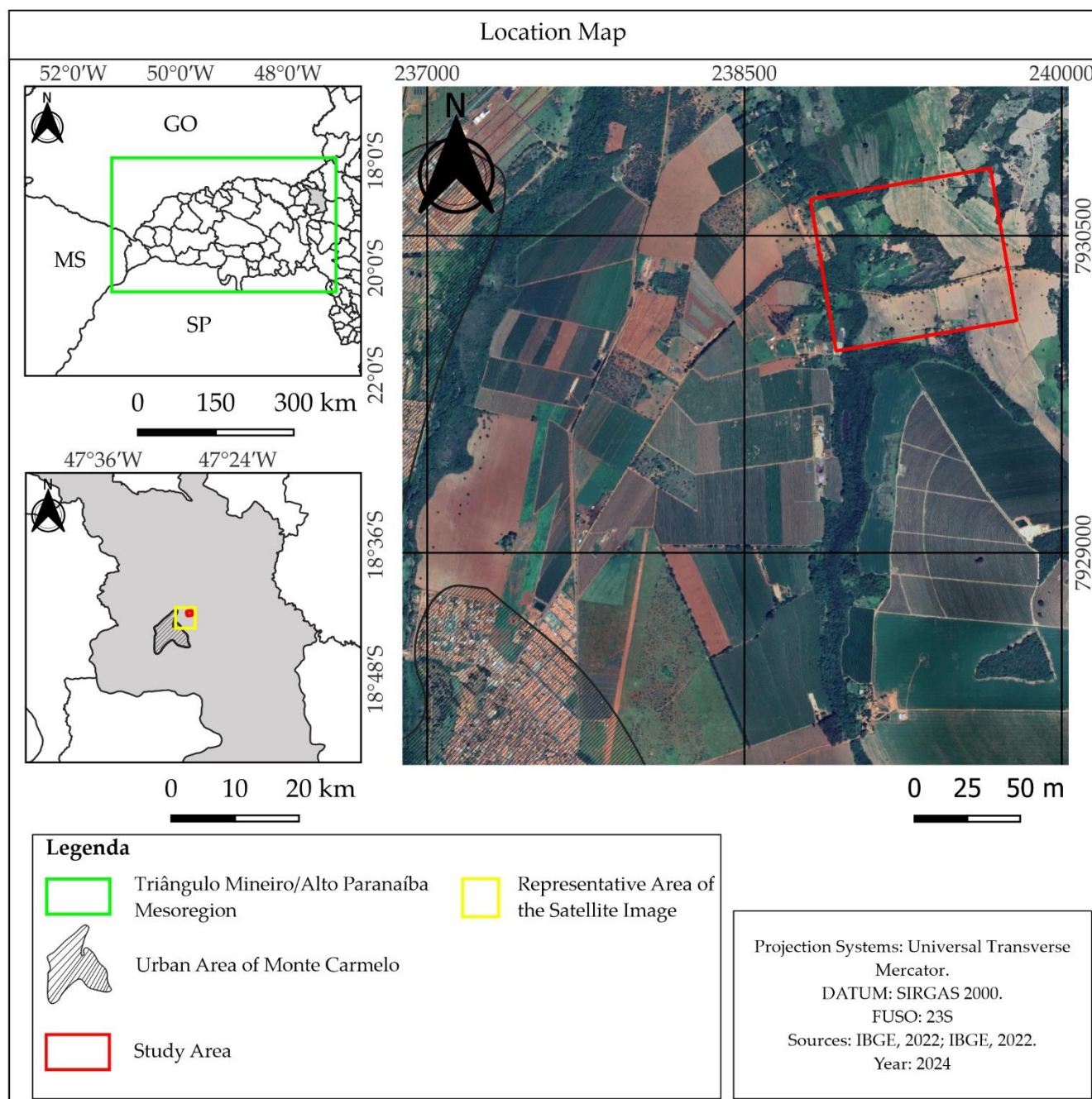


Figure 1. Location of the study area.

Regionally, the area is part of the Cerrado Morphoclimatic Domain (Ab'Sáber, 2003) and corresponds to the morphosculpture of the dissected plateaus of Alto Paranaíba (Rodrigues; Augustin; Nazar, 2023), which are part of the morphostructure of the Brasília Fold Belt (Codemig, 2017). In the region, Latosols, Cambisols and Neosols predominate (Motta; Baruqui; Santos, 2004) under a semi-humid tropical climate (Novais, 2011). In the study area, the presence of Cambisols stands out, recognized in the field by the occurrence of a diagnostic incipient B horizon (Bi). This horizon exhibits little advanced pedogenesis, evidenced by the low development of the soil structure (Embrapa, 2018). According to Arantes (2022), the degree of susceptibility of Cambisols to erosion is related to the proportion of clay, since a lower content of this mineral results in reduced aggregation between larger particles, which makes the soil more prone to removal.

3. Materials and Methods

The methodology for geomorphological mapping was structured in three sequential and integrated stages: pre-field, field and post-field (Table 1). The definition of these stages was based on the demands of the field work, which included the acquisition of RPA images for three scenarios. The resulting detailed geomorphological map constitutes the main product of this work and, together with the field observations, supported the interpretation of the erosion dynamics of the gully.

Table 1. Summary of research steps and procedures.

Stage	Activities and Procedures
Pre-Field	Definition of flight plans
Field	Carrying out aerial surveys with RPA and collecting coordinates with precision GNSS (global navigation satellite system)
Post-Field	Aerial image processing
	Generation of cartographic base and morphometric thematic maps
	Preparation of the detailed geomorphological map
	Selection of Google Earth images to record technogenic deposits

Flight planning began with the delimitation of the study area in Google Earth images and the export of the *Keyhole Markup Language* (KML) file to the *DroneDeploy* application. The three flight plans were prepared with the same parameters of altitude, camera angle and levels of frontal and lateral overlap of the images. The camera angle was adjusted to 90° in relation to the RPA, positioning it perpendicular to the surface. Minimum overlaps of 70% (frontal) and 60% (lateral) were adopted, with a flight altitude of 100 meters in relation to the surface (Figueiredo; Figueiredo, 2018).

Field image acquisition was performed with the RPA DJI Mavic Pro during campaigns in October 2022 and February 2024 (rainy season) and May 2023 (dry season). Reference points were installed concurrently with the flights (Table 1), whose coordinates were obtained in real time (RTK) with a GNSS L1/L2 receiver from the Topography and Geodesy Laboratory (LTGEO IGESC/UFU Monte Carmelo). This procedure aimed to increase the positional and altimetric accuracy of the gully data.

Table 1. Coordinates of reference points (SIRGAS 2000, UTM zone 23 S).

Points	X	Y	Z
1	239465.182	7930491.581	870.294
2	239597.872	7930359.665	869.893
3	239597.872	7930245.269	858.462
4	239202.122	7930203.570	847.633
5	239058.640	7930243.957	846.575
6	239216.640	7930573.958	857.082

The treatment and processing of the RPA images from the campaigns were performed with the Agisoft Metashape software, at the Remote Sensing and Photogrammetry Laboratory (LASER IGESC/UFU Monte Carmelo). In this process, the images were superimposed according to the flight plans (Figure 2) and integrated to generate the orthomosaic and the Digital Terrain Model (DTM). The DTM exclusively represents the terrain elevations, disregarding vegetation and buildings (Figueiredo; Figueiredo, 2018).

According to Oliveira et al. (2017), the generation of the DTM in Agisoft Metashape occurs from the classification of the elements into two categories: ‘ground class’, which contains the terrain points, and ‘non-ground class’, which includes the elements above the surface. After classification and deactivation of the ‘non-ground class’, the DTM is obtained by executing the following sequence of commands in the software: *Workflow > Align Photos; Workflow > Build Dense Cloud; Tools > Classify Ground Points; Workflow > Build Mesh; Tools > Smooth Mesh; and Workflow > Build DEM.*

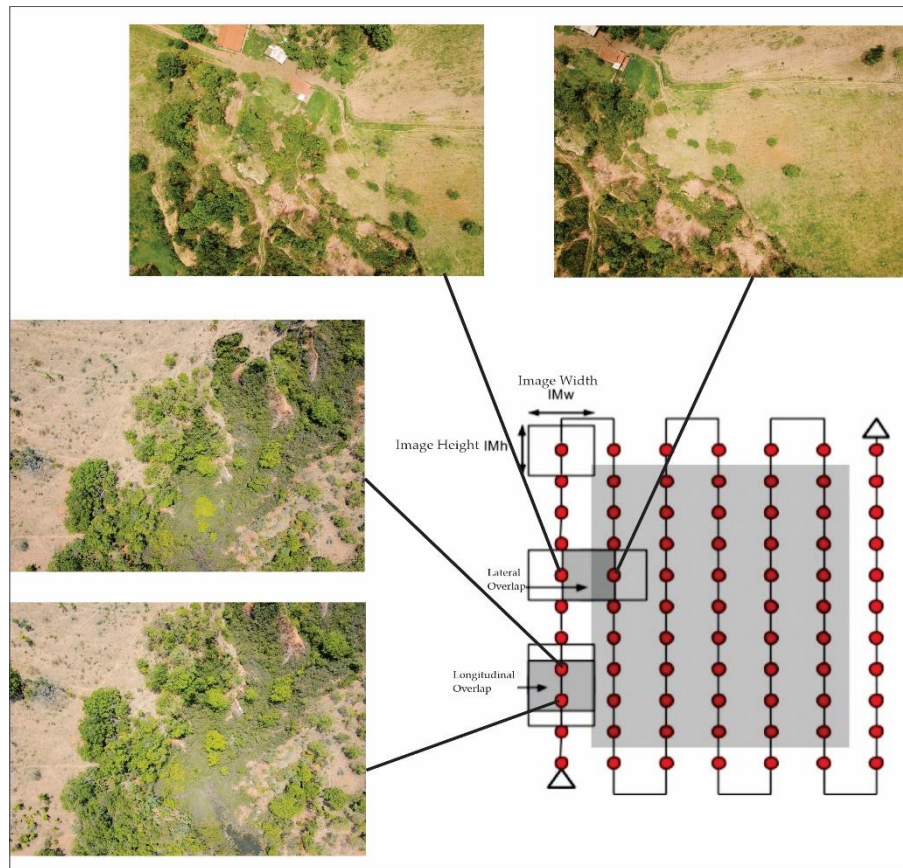


Figure 2. Overlay of aerial photographs acquired through RPA flights for generating orthomosaics. Source: Adapted from PIX4D (2015).

The construction of the orthomosaics (Figure 3) required a change in the point-cloud classification procedure, activating all options for the 'non-soil class'. The command sequence was the same as that used for the DTM, differing only in the final execution of the *Build Orthomosaic* command. The October 2022 orthomosaic served as the basis for the cartographic organization, and the contour lines were extracted from the DTM using the *Tools > Generate Contours* command. Subsequently, the vectorization of fluvial and pluvial channels, impoundments, and access roads was carried out through photointerpretation of the images. All processing for the preparation of the cartographic basemap and the morphometric and geomorphological maps was performed in the QGIS 3.22.16 software, at a scale of 1:7,000.

The hypsometric map, which represents the altimetry classes, was prepared from the DTM. For this, the data were grouped into nine classes with five-meter intervals: <801 m; 805–810 m; 810–815 m; 815–820 m; 820–825 m; 825–830 m; 830–835 m; 835–840 m; and >840 m. Similarly, the slope map, which expresses the slope gradient, was generated from the DTM. The slope classes, with intervals of 0–2%, 2–5%, 5–12%, 12–30%, 30–45%, and >45%, were based on Silva and Lupinacci (2021). These products, together with the photointerpretation of the three aerial surveys, supported the preparation of the detailed geomorphological map.

To prepare the geomorphological map, preference was given to images from the May 2023 aerial survey. Collection during the dry season provided greater clarity and visual resolution. At this stage, the gully was compartmentalized and the denudational and aggradational features within each compartment were identified. The following compartments were defined (Figure 4):

- Dissected Area: located inside the gully, it represents the actively eroded compartment that houses the fluvial and pluvial channels.
- Hillslopes Directed towards the Gully: correspond to all the surrounding areas that drain towards the main erosive feature or the Fluvial Plain and Terrace (Aptf) of the Mombuca stream.

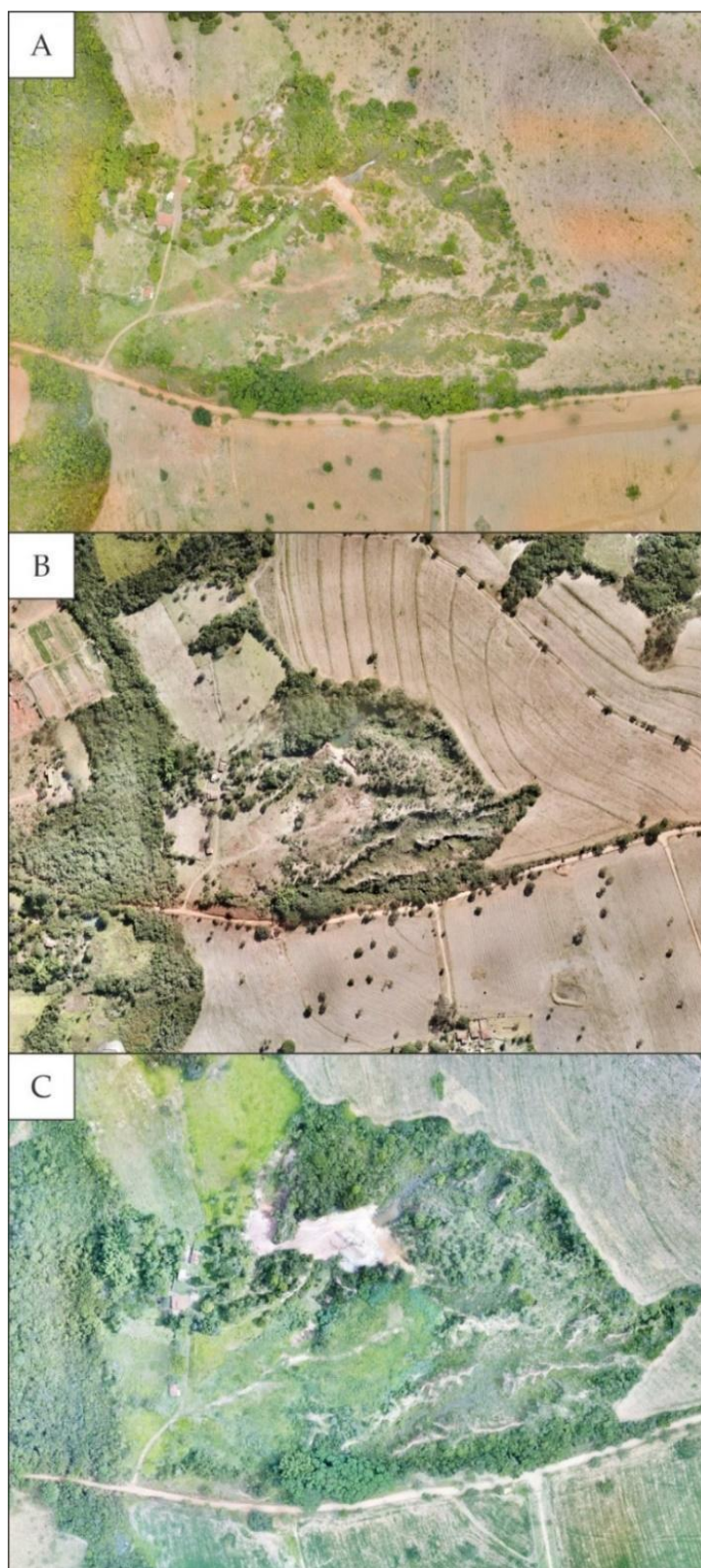


Figure 3. Orthomosaics generated for the study area. Campaigns: A - Oct/2022; B - May/2023; C - Feb/2024.

- Residual Landforms Connected to the Hillslopes Directed towards the Gully: constitute subtle connections between the recesses of the erosional edge and the residual landforms of the Dissected Area.
- Residual Landforms Not Connected to Hillslopes: located inside the Dissected Area and present topographic levels similar to those of the Connected Residual Landforms.

- Accumulation of Fluvial Plains and Terraces (Aptf): corresponds to areas of deposition and accumulation of alluvial sediments. They are found mainly along the Mombuca stream, where the gully channels flow into, and in smaller portions within the Dissected Area.

The individualized denudational features (Figure 5) were categorized and interpreted as follows:

- Erosional Edge: feature that delimits the compartments of Hillslopes Directed towards the Gully, Connected Residual Landforms and Dissected Area.
- Old Erosional Edge: corresponds to the relief ruptures in the Residual Landforms Not Connected compartment.
- Piping: features located on the walls of the erosional edge, which constitute subsurface erosion ducts observed in the field.
- Edge Deposit: features that occur on the erosional edge, accumulated predominantly at the base of the wall. They derive from the detachment and deposition of materials more susceptible to erosion at the foot of the slope.
- Topographical ruptures: abrupt differences in level located on the hillslopes.
- Rills: linear erosion features resulting from surface runoff.

The representation of individualized features in the geomorphological compartments (Figure 4) used symbols consolidated in detailed cartography (Figures 4 and 5). The symbols for Pluvial and Fluvial Channels, Road Cuts and Agricultural Terraces from Tricart (1965) and for Flat-bottomed Valley, V-shaped incised Valley, Topographic Rupture and Rills from Verstappen and Zuidan (1975) were adopted. Additionally, the symbol for Infilled Original Drainage proposed by Silveira and Cunha (2012) was used.

Given the lack of specific symbols for some gully features, adaptations were made based on the literature. The Erosional Edge symbol was adapted from the Topographic Rupture of Verstappen and Zuidan (1975); the Old Erosional Edge symbol was adapted from the Symmetric Crest of IBGE (2009); the Edge Deposit symbol was adapted from the Mass-Movement symbol of IBGE (2009); and the Rural Buildings symbol was adapted from the model of Silva, Silveira and Barbosa (2023).

Additionally, historical satellite images of the area were selected to determine the years of emergence of technogenic deposits and the clogging of old fluvial channels of the gully. For this analysis, images from the years 2007, 2016, 2017, 2018 and 2019, obtained from the Google Earth platform, were mainly used. The expansion of technogenic deposits throughout the investigated period was recorded by means of polygons with red color intensity (Figure 4). The resulting shapes of these deposits were also evaluated according to the classification of Moura et al. (2023).

4. Detailed morphometric and geomorphological mapping

From the regressive erosional fronts of the mapped gully, fluvial channels with an E-W orientation depart and head towards the Mombuca stream, whose flow follows the S-N direction (Figure 6). The elevations in the mapped area range from values below 805 m to values above 840 m (Figures 7 and 8). In the gully sector, the elevations vary between 815 m and 840 m, which represents a drop of 25 m for the erosion feature. On the convex tops, the slope classes of 0–2% and 2–5% predominate, while on the upper hillslopes the slope increases to 5–12% (Figure 9). On the middle hillslopes, where the erosion feature is installed, the classes reach higher values (12–30%, 30–45% and >45%). At the bottom of the valley, in turn, the gradient decreases again, presenting classes of <2%, 2–5% and 5–12%.

Five geomorphological compartments were defined for the studied gully. In these compartments, the individual features and the gradual advancement of the technogenic deposits were cartographically recorded (Figure 10). The detailed geomorphological map (Figure 10) consists of hatched polygons that represent the five compartments and the technogenic deposits (in a red gradient). The map also includes lines and point symbols that indicate topographic data, incised landforms, denudational features and anthropogenic landforms (Figure 11).


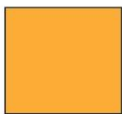

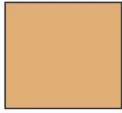







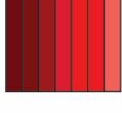

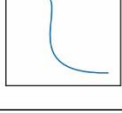

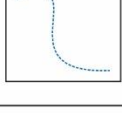

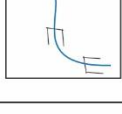

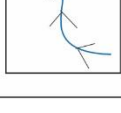
Compartments and Mapped Features		RPA Images	Polygons and Symbols	Sources
Gully Compartment	Dissected Area			Cartographic Convernion
	Hillslopes Directed Towards the Gully			Cartographic Convernion
	Residual Landforms Connected to Hillslopes Directed Towards the Gully			Cartographic Convernion
	Residual Landforms not Connected to Hillslopes			Cartographic Convernion
	Aptf (Fluvial Plains and Terraces)			Adapted from Tricart (1965)
Technogenic Deposits				Cartographic Convernion
Flowing water and incised landforms	Fluvial Channel			Cartographic Convernion/ Tricart (1965)
	Pluvial Channel			Cartographic Convernion/ Tricart (1965)
	Flat-Bottomed Valley			Verstappen and Zuidan (1975)
	V-Shaped Incised Valley			Verstappen and Zuidan (1975)

Figure 4. Structure of the legend that makes up the detailed geomorphological map of the Mombuca gully.


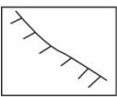

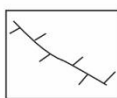



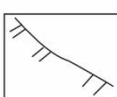





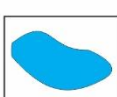



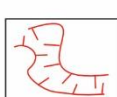






Compartments and Mapped Features		RPA Images	Polygons and Symbols	Sources
Denudational Features	Erosional Edge			Adapted from Topographic Rupture Feature by Verstappen and Zuidan (1975)
	Old Erosional Edge			Adapted from the IBGE Symmetrical Crest Feature (2009)
	Edge Deposit			Adapted from the IBGE Mass-Movement Phenomena Feature (2009)
	Topographic Rupture			Verstappen and Zuidan (1975)
	Rills			Verstappen and Zuidan (1975)
Anthropogenic Landforms	Impoundments			Cartographic Convention
	Agricultural Reservoir			Cartographic Convention
	Roads			Cartographic Convention
	Road Cuts			Tricart (1965)
	Agricultural Terraces			Tricart (1965)
	Infilled Original Drainage Channels			Silveira and Cunha (2012)
	Rural Building			Adapted from Silva, Silveira and Barbosa (2023)

Figure 5. Structure of the legend that makes up the detailed geomorphological map of the Mombuca gully.

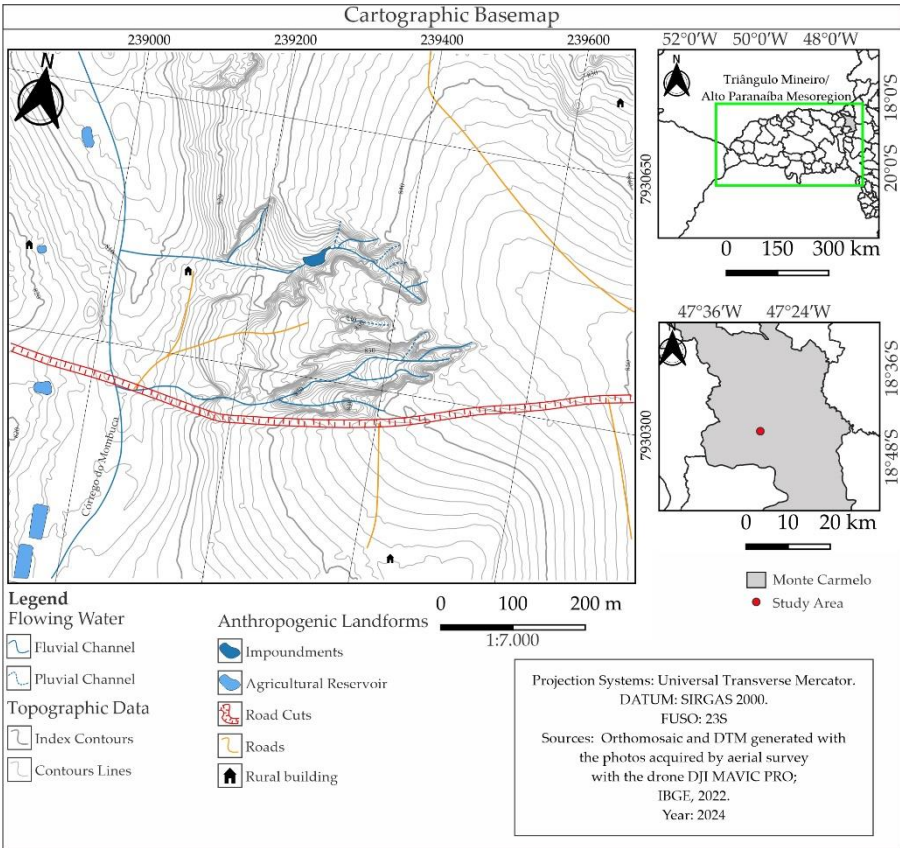


Figure 6. Cartographic basemap of the study area.

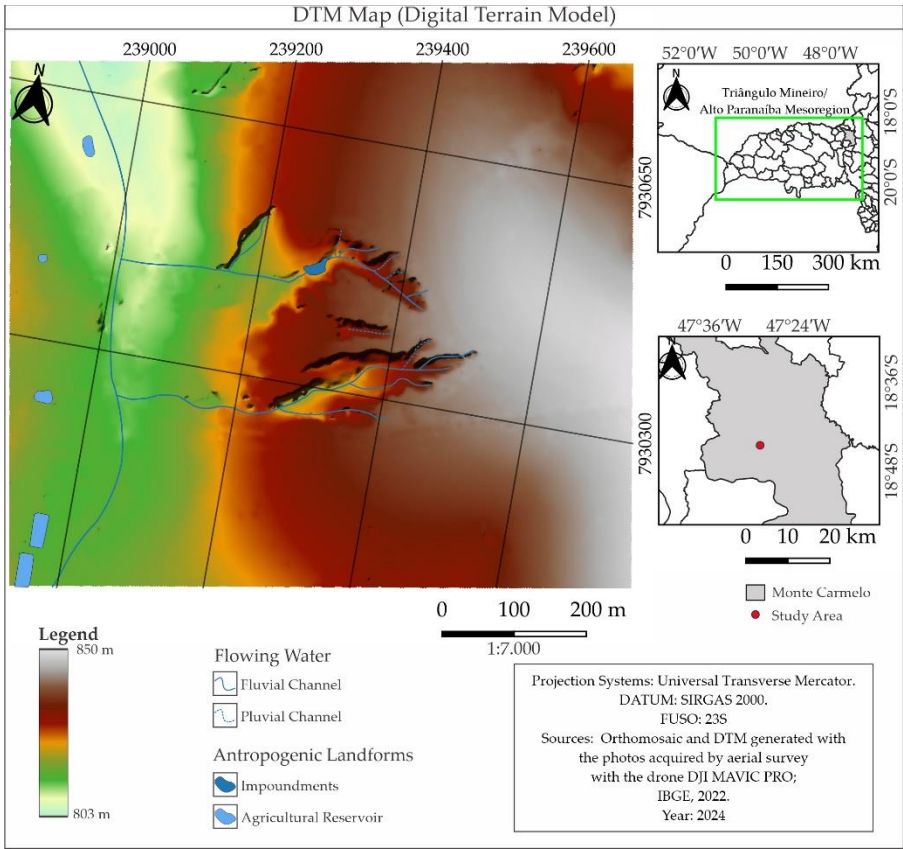


Figure 7. DTM of the study area.

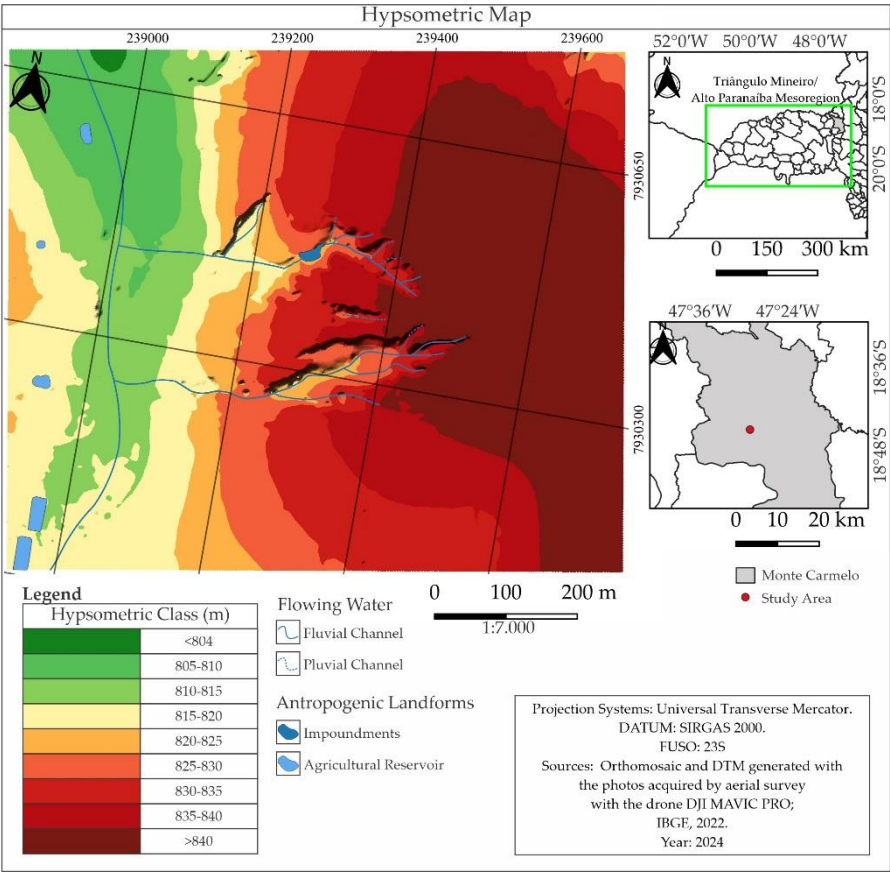


Figure 8. Hypsometric map of the study area.

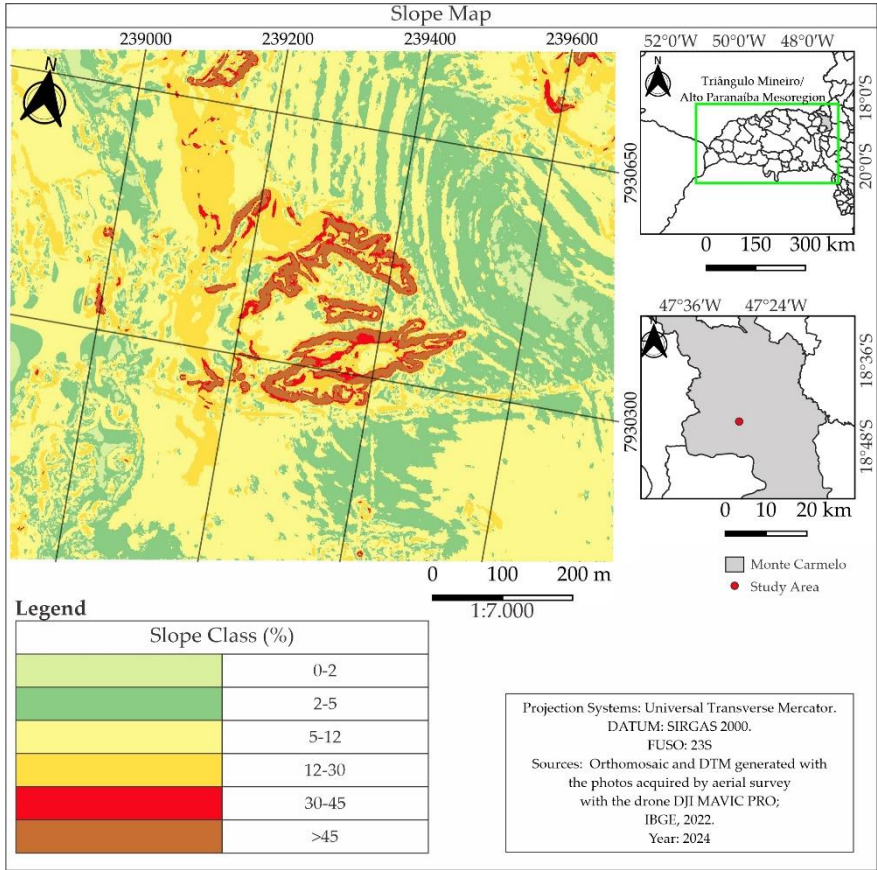


Figure 9. Slope map of the study area.

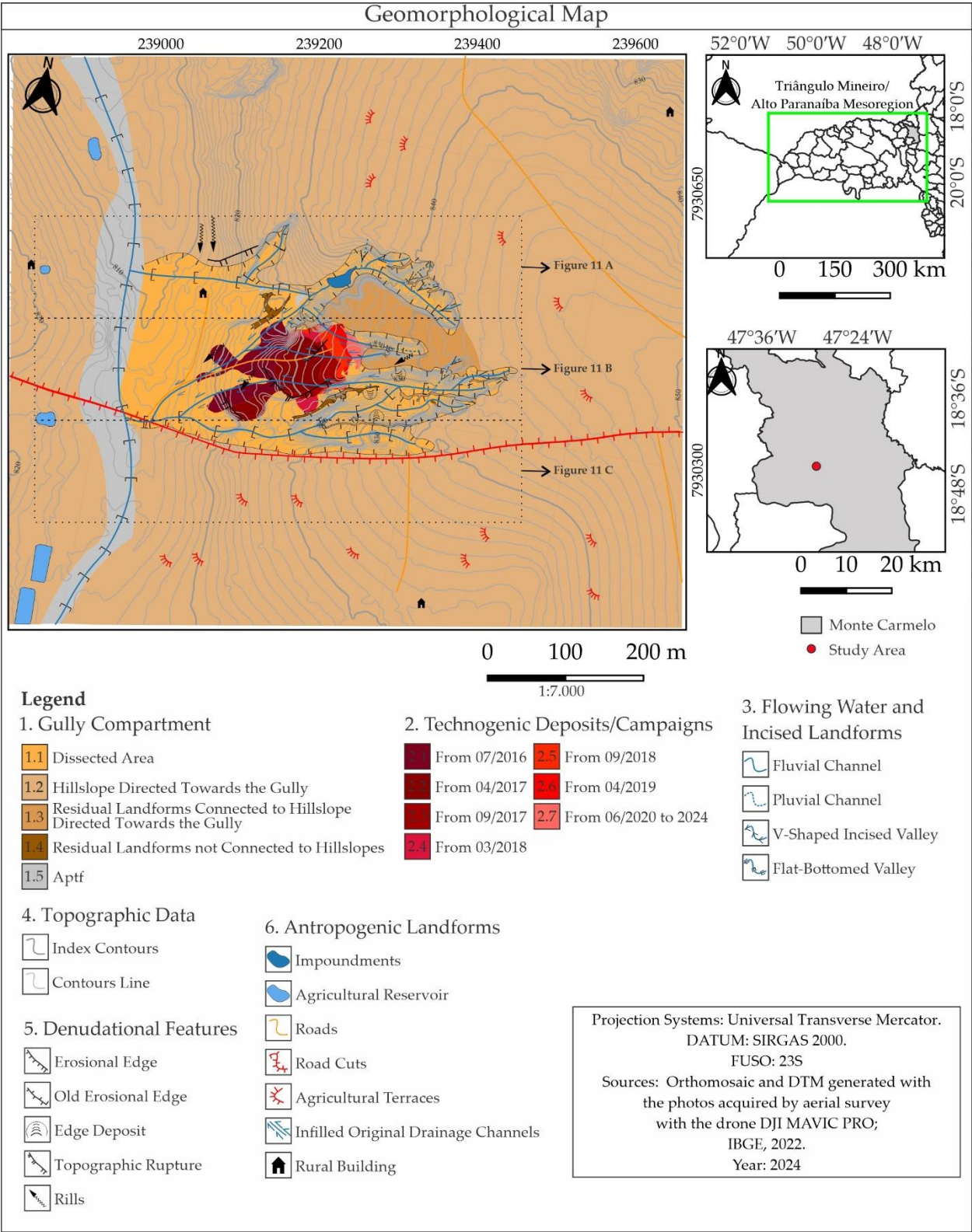


Figure 10. Detailed geomorphological map of the study area.

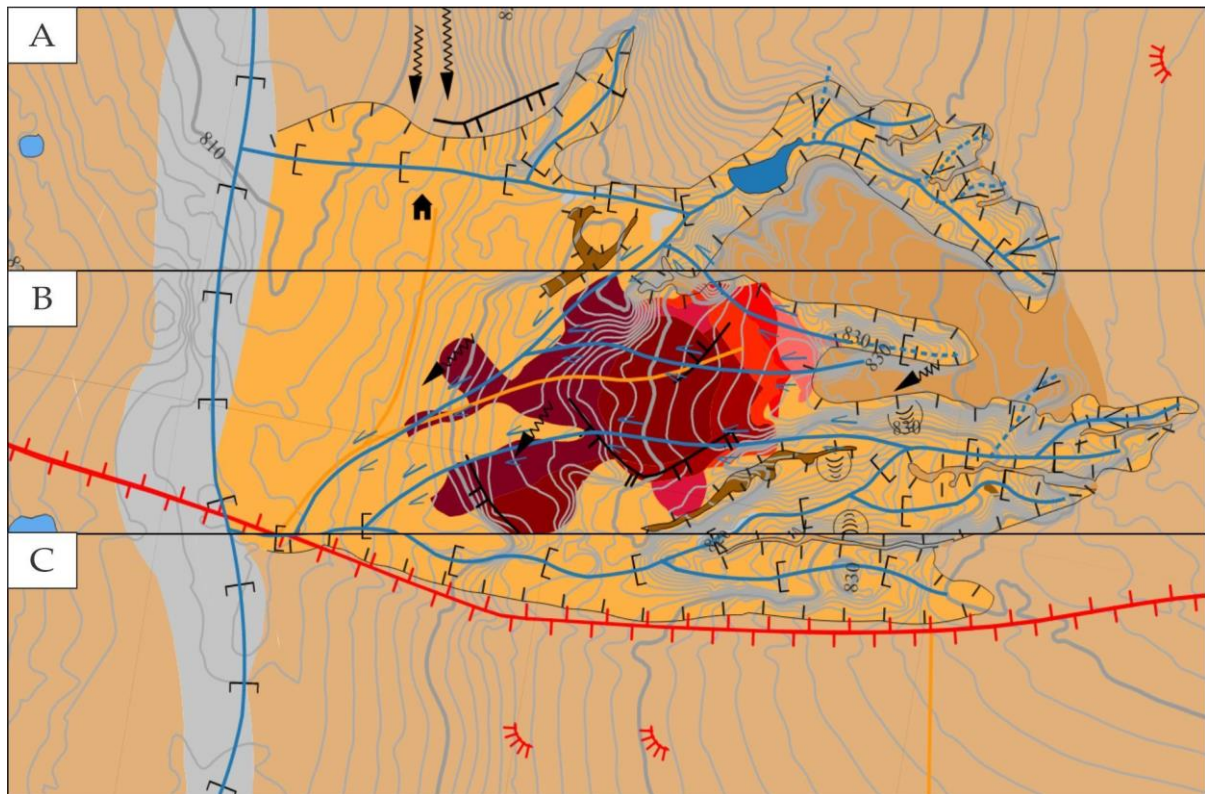


Figure 11. Fragments and enlargement of the detailed geomorphological map, consisting of polygons (geomorphological compartments and technogenic deposits), lines and point symbols (topographic data, flowing waters and incised landforms, denudation features and anthropogenic landforms). The legend for this figure can be found in Figures 4, 5 and 10.

The Mombuca gully presents three main erosional fronts (Figure 12), with the retreat of channel 1 towards the SE (Figure 13 A) and channels 2 and 3 towards the E (Figures 13 B and C). This dynamic indicates a possible future connection between the fronts, if the retreat persists. The intensity of the erosion dynamics is evidenced by the denudational features identified in the geomorphological compartments (Figure 10). These features were documented in the field and include: erosional edge (Figure 13 D), old erosional edge (Figure 13 E), piping (Figure 13 F), edge deposit (Figure 13 G), topographic ruptures (Figure 13 H) and rills (Figure 13 I). The materials from this dynamic are transported and deposited in the river channels, where they form Accumulations of Fluvial Plains and Terraces (Aptf) inside the gully (Figure 13 J).

The joint analysis of images from different periods, obtained from Google Earth and the three aerial surveys with RPA, allowed the identification of human interventions in the area. Such actions occurred especially inside the gully and include the change in the orientation of the flow of the channels, the construction of impoundments and the filling with technogenic deposits (Figure 14).

In 2007, the gully showed little human interference inside it, with the exception of a rural building near the canal outlet, while the surrounding area was already occupied by agricultural activities (Figure 14 A). In 2013, an impoundment was constructed in a channel adjacent to the gully, on a hillslope that also drains into the Mombuca stream (Figure 14 B). The year 2016 marked the intensification of human actions inside the erosional feature, with the filling of channels by technogenic deposits and the change in the direction of the water flow (Figure 14 C). In the 2022 campaign, the filling of channel 3 by technogenic deposits (Figure 12) is observed, especially in the central portion of the gully, and a significant change in the direction of water flows (Figure 14 D). During this same period, the existence of an impoundment in channel 1 was noted (Figures 10 and 12).

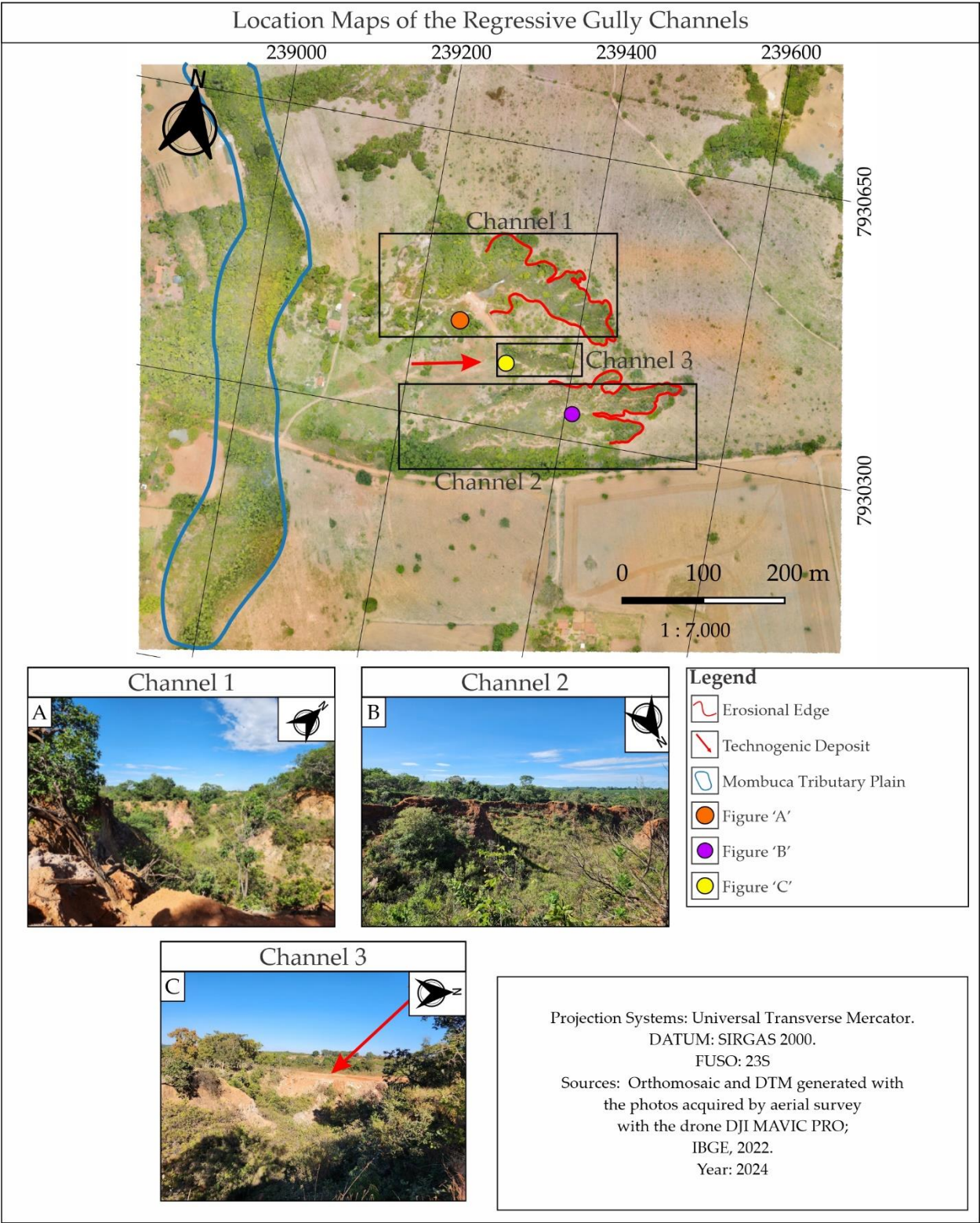


Figure 12. Identification of erosional fronts created by channels. A: channel 1; B: channel 2; C: channel 3.

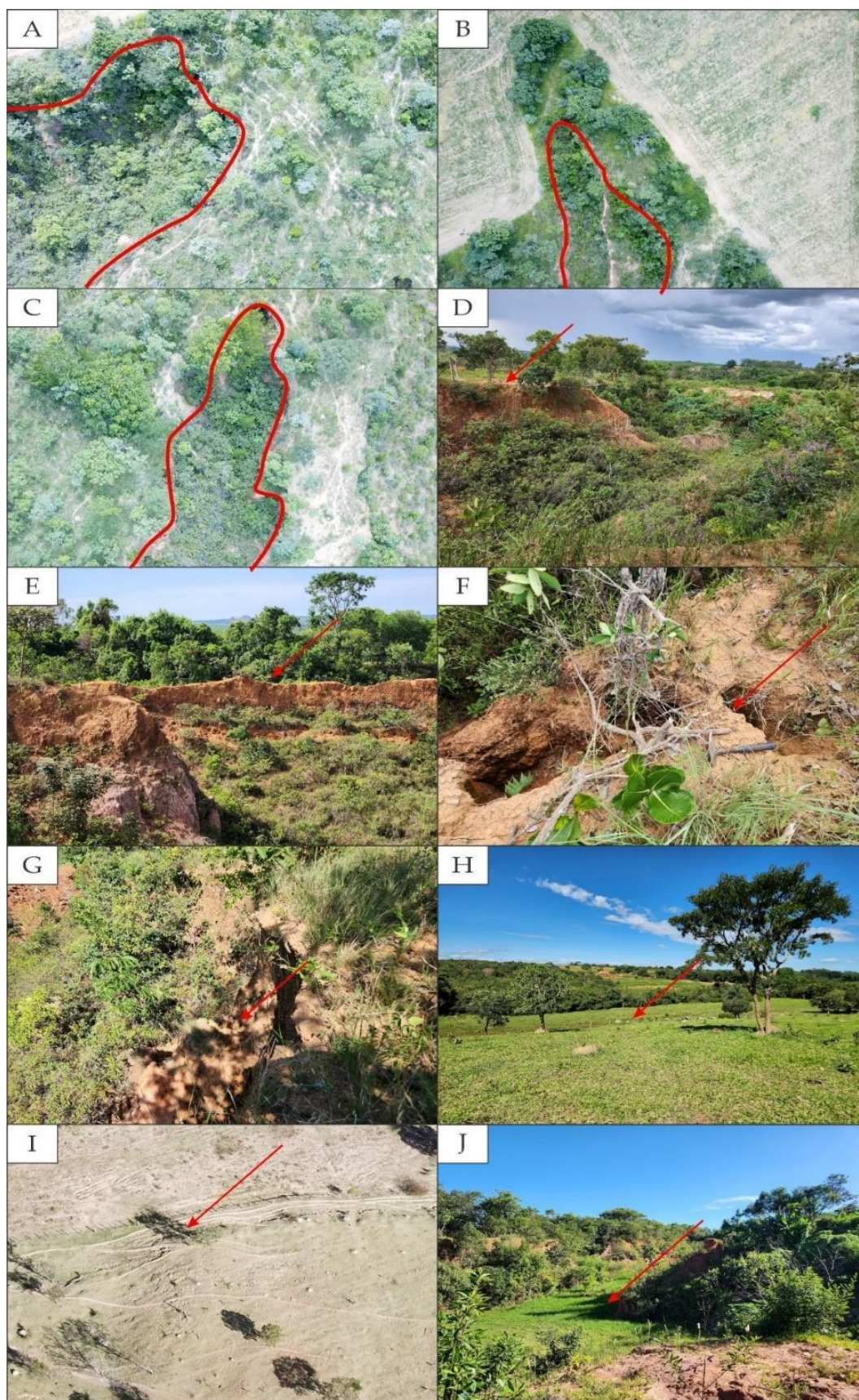


Figure 13. A, B and C: Three erosional fronts present in the gully (A: Channel 1; B: Channel 2 and C: Channel 3); D: Erosional Edge; E: Old Erosional Edge; F: Piping; G: Edge Deposits; H: Topographic Rupture; I: Rills; J: Aptf inside the gully.

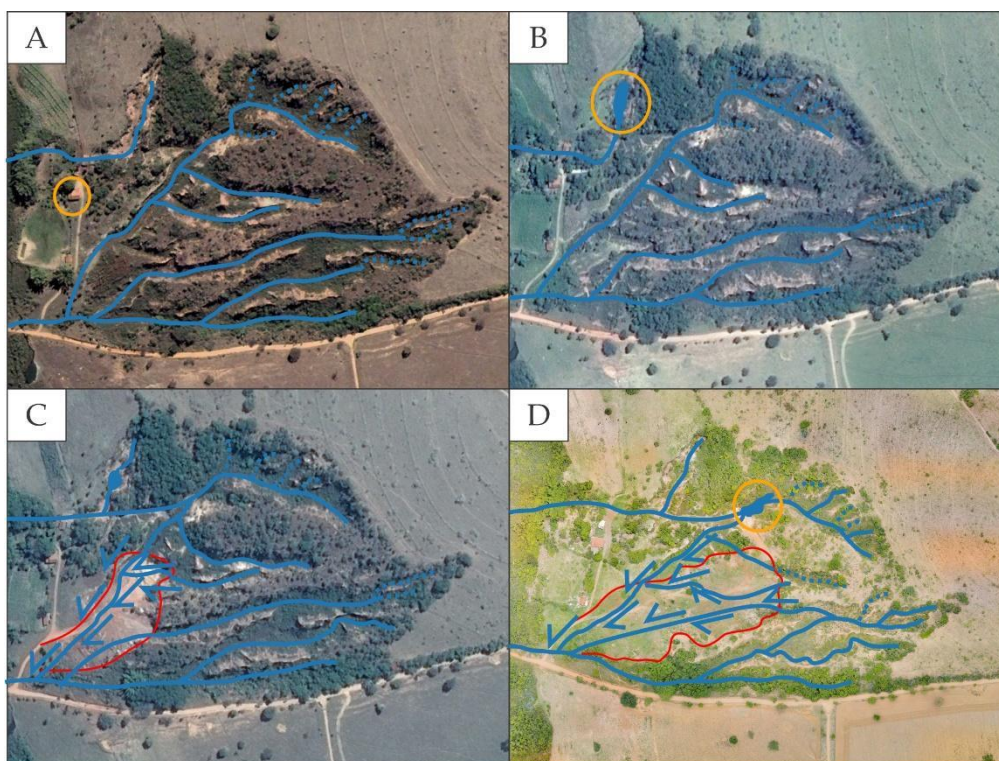


Figure 14. A: Scenario of the gully in 2007 (highlighting the constructed rural building); B: Campaign of the gully in 2013 (highlighting the impoundment built in a channel positioned to the right of the gully); C: Campaign of the gully in 2016 (highlighting the infilling of channels and change in the orientation of the water flow); D: Campaign of the gully in 2022 (highlighting the infilling by technological deposits of channel 3 with significant change in the orientation of the water flows). Source: A, B and C: Google Earth; D: RPA image (campaign October/2022).

During the period investigated by this study (2022 to 2024), the expansion of the infilling front by technogenic materials was observed, especially in channel 3. The RPA image from October 2022 (Figure 15 A) shows the expansion front of the deposits, which were also recorded in the field (Figure 15 B). The comparison between the RPA images from October 2022 (Figure 15 A) and May 2023 (Figure 15 C) reveals the expansion of the technogenic infilling, a fact confirmed by field records (Figure 15 D). In the image from February 2024 (Figure 15 E), no significant expansion of the deposit front was observed. However, an increase in vegetation density was observed due to the rainy season (summer) (Figure 15 F). According to the classification proposed by Moura et al. (2023), the technogenic landform resulting from the accumulation of materials in channel 3 is categorized by Technogenic Elevation and Superposition of the Accumulation Technoform type.

The construction of an impoundment inside the gully constitutes another relevant human intervention in the study area. In the October 2022 RPA image (Figure 16 A), the dam installed in channel 1 (Figure 12) is evident, in a segment with a high degree of drainage incision (Figure 16 B). The comparison between the October 2022 (Figure 16 A) and May 2023 (Figure 16 C) images indicates the loss of dam material. This loss was due to the formation of erosional rills by the action of pluvial runoff, as recorded in the field (Figure 16 D). The February 2024 image (Figure 16 E) shows a significant remobilization of dam materials, with the formation of erosional rills and ravines. Field investigation revealed that materials (soils and saprolites) were removed from the erosional edge to be used in the compaction and support of the dam (Figure 16 F). However, with the rains at the end of 2023, the materials that make up the dam embankment underwent an intensification of linear erosion processes. Due to the upheaval of materials for the construction of the dam, this technogenic form would be categorized as Technogenic Corrugation of the Turbation Technoform type (Moura et al., 2023).

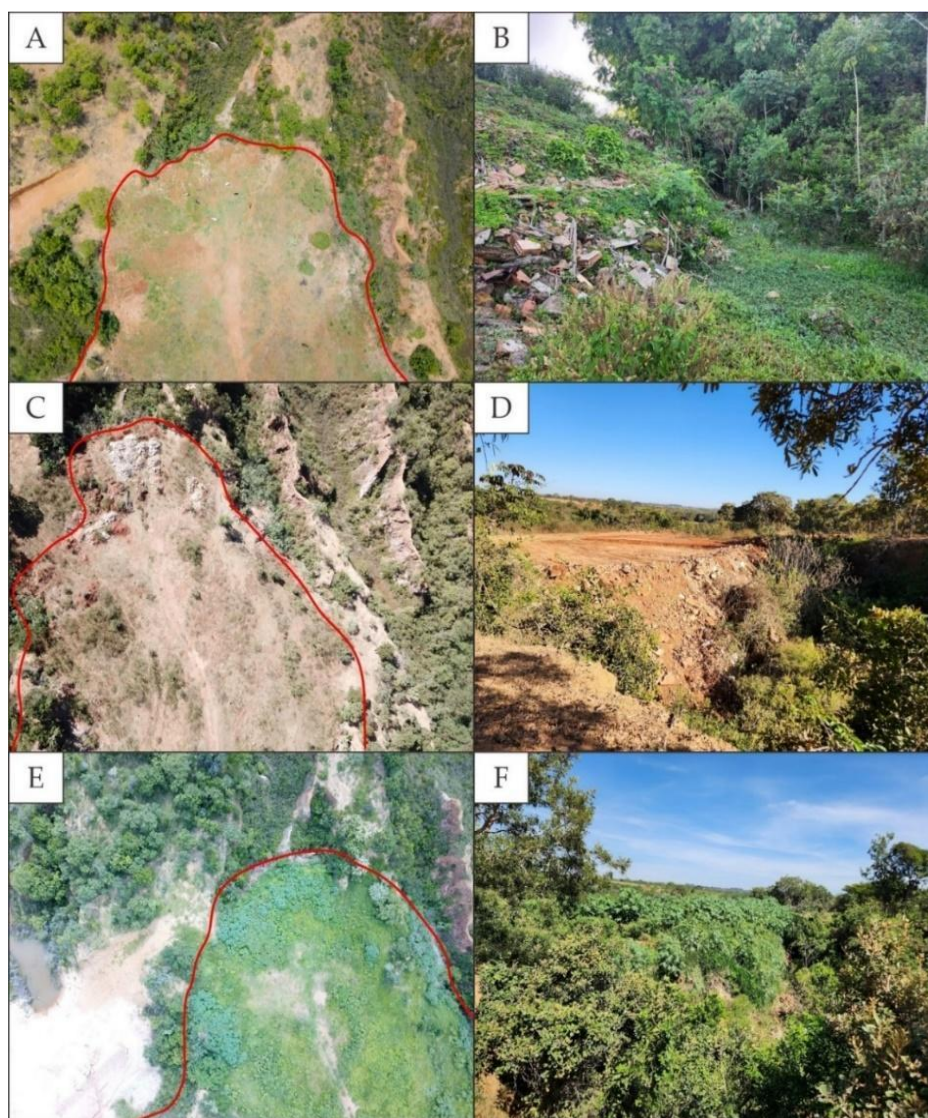


Figure 15. A and B: RPA image and field record, Oct/2022; C and D: RPA image and field record, May/2023; E and F: RPA image and field record, Feb/2024. The red lines in the images indicate the limits of the expansion fronts of the technogenic deposits.

5. Geomorphological compartments and individualized features

Table 2 summarizes the information obtained in this study for the five geomorphological compartments defined in the Mombuca gully (Figure 10). The Dissected Area compartment (1.1) (Figure 10) has morphometric characteristics that indicate a high potential for erosion dynamics (Figures 7, 8 and 9). This potential is confirmed by the record of denudational features, such as topographic ruptures and rills. The incised landforms of the fluvial and pluvial channels are predominantly “V” valleys, with occasional occurrences of flat-bottomed valleys. The anthropogenic landforms include technogenic deposits (Figure 15), impoundments (Figure 16), infilled original drainage (Figures 14 C and D) and rural buildings (Figure 14 A).

Channels 1 (Figures 17 A and B) and 2 (Figures 17 C and D) are mainly responsible for the dissection of this compartment. However, between these two main channels, a third channel was identified (Figures 17 E and F), currently disconnected from the others. The infilling of this third channel with technogenic deposits (Figure 14 D) interfered with the values recorded by the hypsometry, DTM and slope mappings (Figures 7 to 9). In the area infilled by these deposits (Figure 15), the hypsometry and DTM values increased, while those of slope decreased. This result contradicts the natural incision dynamics of the drainage network in the gully process.

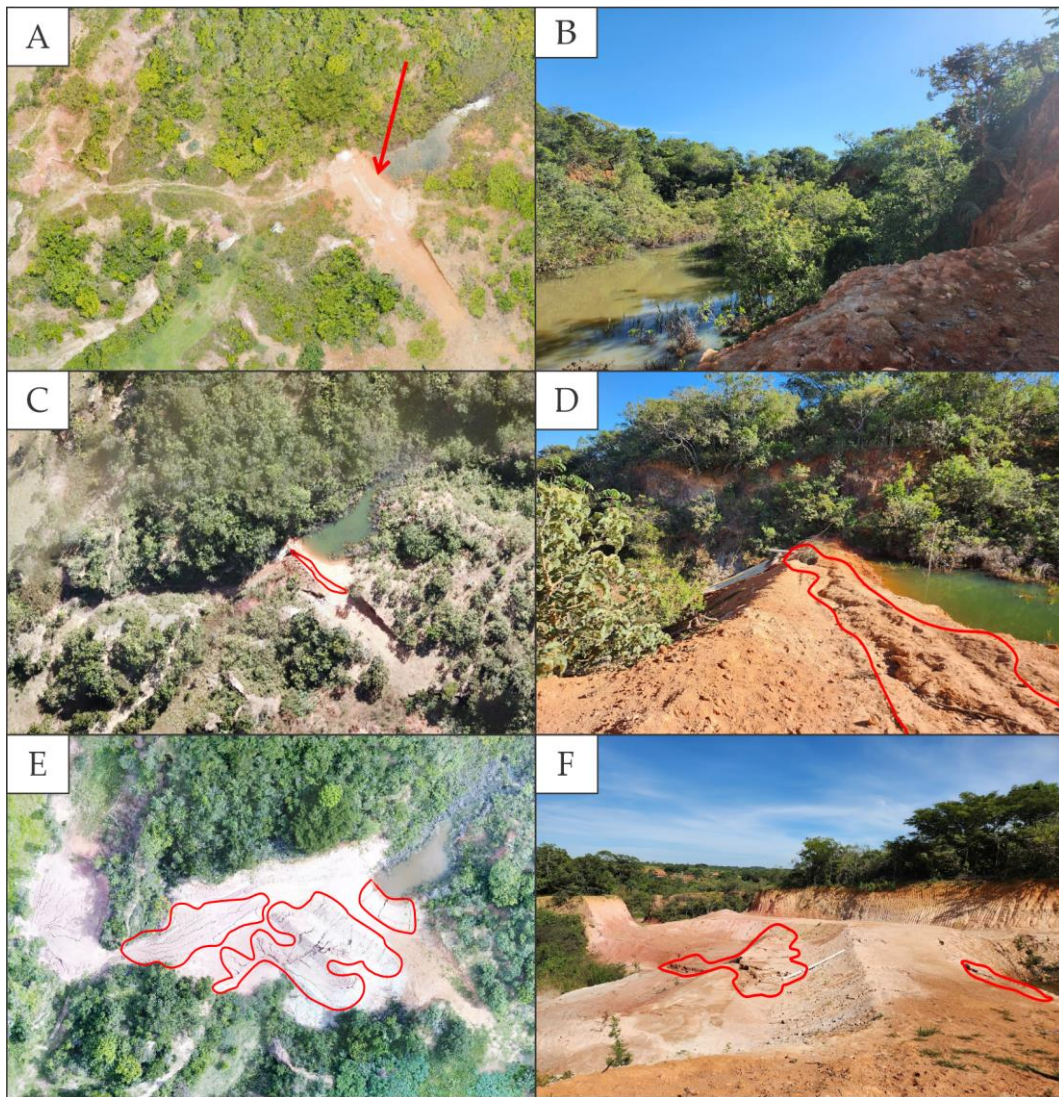


Figure 16. A: Channel 1 impoundment, RPA image from 2022; B: Channel 1 impounded and erosional edge in the background (2022); C: Channel 1 impoundment, RPA image from 2023; D: Infill of the channel 1 impoundment with linear erosion (2023); E: Channel 1 impoundment, RPA image from 2024; F: Enlargement of the linear erosion of the infill of the channel 1 impoundment (2024).

The infilled channel (3) originally connected to channel 1 of the gully (Figure 14 A). With the expansion of the technogenic infilling (Figure 15), the orientation of the original watercourse was changed (Figures 14 C and D). The geomorphological map (Figure 10), through the red color gradient, records the moment when the gully underwent intensification of the technogenic infilling (July 2016) and highlights the subsequent years of expansion of this anthropogenic deposition.

The compartment of the Hillslopes Directed towards the Gully (1.2) is the largest in the studied area, since it covers the entire area surrounding the feature, upstream of the erosional edge. Due to its greater scope, it presents a variety of altimetric and hillslope gradient classes, although these are predominantly lower than those of the compartment of the Dissected Area (1.1). The denudational features include topographic ruptures (Figure 13 H) and rills (Figure 13 I). The anthropogenic landforms, in turn, correspond to reservoirs for agricultural use, terraces, rural buildings, roads and road cuts (Figure 11). The presence of these models indicates the intense agricultural activity in the area surrounding the gully.

The compartment of Residual Landforms Connected to Hillslopes (1.3) exhibits intense erosive action, although it remains subtly interconnected to the compartment of Hillslopes Directed towards the Gully (1.2). This compartment has pronounced morphometric characteristics, which are concentrated mainly in the hillslope segment that marks the transition to the Dissected Area (1.1). Such characteristics correspond to the denudational

forms of the erosional edges (Figure 13 D), which delimit the gully from the adjacent areas susceptible to regressive erosion (1.1).

Table 2. Summary of information acquired from geomorphological compartments.

Compartments	Hypsometric Class (m)	Slope Class (%)	Denudational Features	Flowing Water ^e Incised Landforms	Anthropogenic Landforms
1.1-Dissected Area	804; a 840.	2-5; 5-12; 12-30; 30-45; >45	Topographic Rupture; Rills	Fluvial Channel; Pluvial Channel; V-Shaped Incised Valley; Flat-Bottomed Valley.	Technogenic Deposits; Impoundments; Infilled Original Drainage Channels; Rural Building.
1.2-Hillslopes Directed Towards the Gully	804 a 850	0-2; 2-5; 5-12;	Topographic Rupture; Rills	Fluvial Channel	Agricultural Reservoir; Roads; Roads Cuts; Agricultural Terraces; Rural Building
1.3-Residual Landforms Connected to Hillslopes Directed Towards the Gully	820 a 840	5-12; 12-30; 30-45; >45	Erosional Edge; Edge Deposit; Rills; Piping	Pluvial Channel	X
1.4-Residual Landforms not Connected to Hillslopes	820 a 840	5-12; 12-30; 30-45; >45	Old Erosional Edge; Edge Deposit; Piping	Pluvial Channel	X
1.5-Aptf	804 a 825	0-2 2-5	X	Fluvial Channel; Flat-Bottomed Valley.	X

Denudation features such as edge deposits (Figure 13 G), which are sites of accumulation of material from edge erosion, and piping (Figure 13 F), and manifests itself as subsurface ducts in the wall of the erosional edge, are also recorded in this compartment. According to Augustin and Aranha (2006), ducts formed by piping are subsurface erosion features present in various types of climates. Specific literature attributes a significant participation in the development of gullies to these ducts. Such features have only been identified in the field, where they occur in large quantities and are responsible for the retreat of the edge.

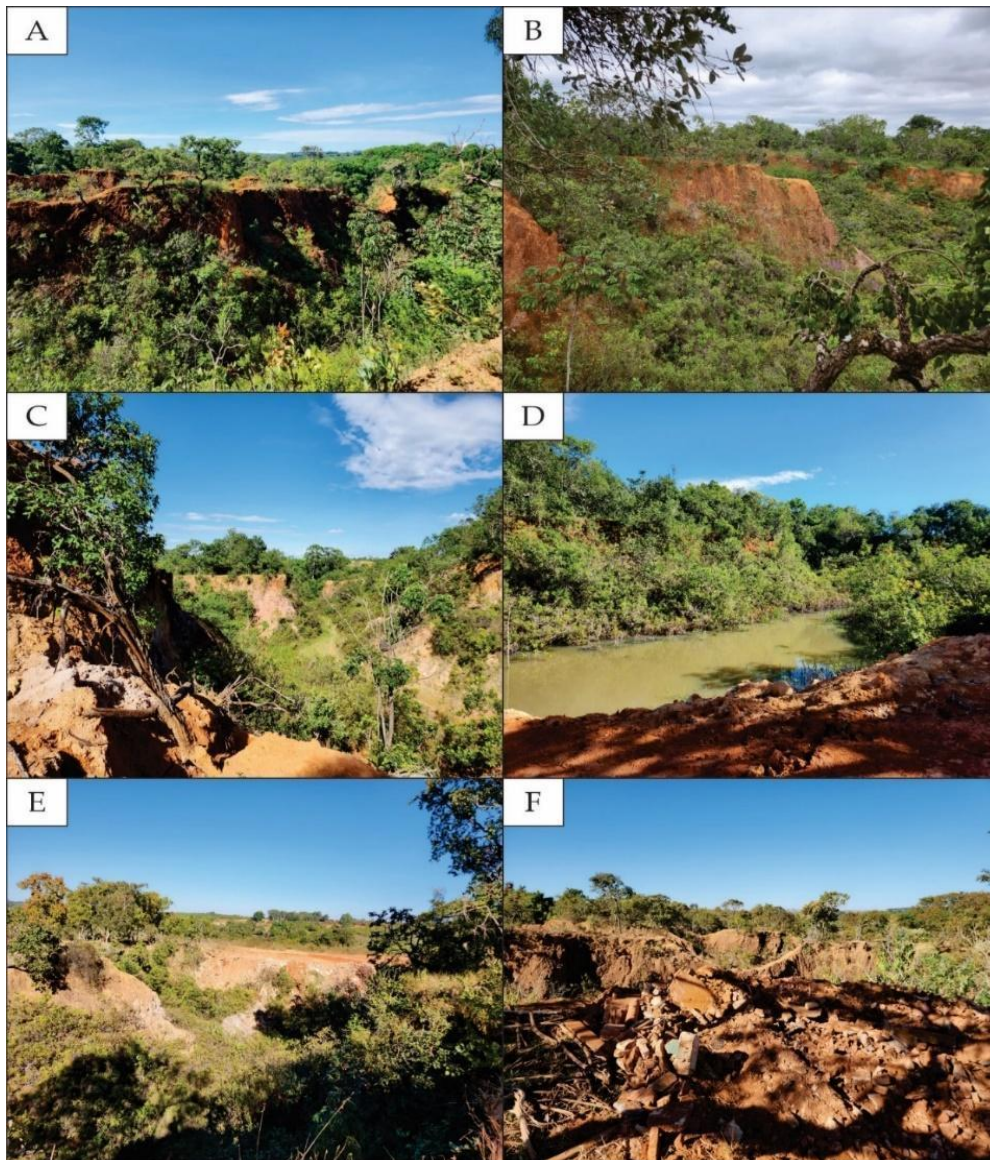


Figure 17. A and B: Channel 1; C and D: Channel 2; E and F: Channel 3, with technogenic deposit.

The compartment of Residual Landforms Not Connected to Hillslopes (1.4) presents morphological and morphometric characteristics similar to those of the Connected Residual Landforms (1.3). However, it is no longer interconnected to the compartment of Hillslopes Directed towards the Gully (1.2) and is positioned in a more internal area of the Dissected Area (1.1). The similarity extends to the incised landforms, with the presence of fluvial channels in valleys with a “V” profile. Regarding the recorded denudational features, the main difference is the presence of the old erosional edge (Figure 13 E). This consists of relief ruptures that mark the limit of terrains with greater relative resistance to erosion, which are no longer connected to the Hillslopes Directed towards the Gully (1.2).

The last defined compartment, Accumulation of Fluvial Plains and Terraces (Aptf) (1.5), exhibits reduced altimetric and slope variation. The incised landforms correspond to fluvial channels with flat-bottomed valleys, a feature resulting from the accumulation of sediments from the erosion processes of the upstream compartments (Figure 13 J). In the surroundings of the fluvial channel of the Mombuca stream, hydromorphic soils with the presence of buriti palms were observed, which characterizes the local ecosystem as a *vereda*. It is noted that these areas have been suffering degradation due to human action.

6. Conclusions

Given the expansion of geomorphology studies applied to gullies using RPA images, this study developed a detailed geomorphological mapping. The objective was to represent the compartmentalization of the gully and record the individualized denudational and aggradational features within and around it, using both traditional and adapted symbols from geomorphological cartography. For this purpose, the Mombuca gully was selected, located near the urban perimeter of Monte Carmelo, because it presents intense interference from human action in its dynamics.

Detailed geomorphological mapping recorded, through polygons, five compartments for the gully and the evolution of technogenic deposits, which intensified from 2016 onwards. Additionally, the mapping documented the change in the orientation of original fluvial courses and the installation of an impoundment. Furthermore, in the five geomorphological compartments, specific features were recorded through symbolologies that evidence the regressive erosion of two main erosional edges.

The Mombuca gully was formed by the linear erosion of fragile materials (Cambisols and saprolites) derived from the granite of the Monte Carmelo Complex. These materials are subject to surface runoff under tropical climate conditions, which carves the channels, reaches the subsurface waters and increases regressive erosion. The fragility of the materials and the climate regime are compounded by human actions. Despite the presence of mapped agricultural terraces in the surrounding area, the occurrence of diffuse runoff and rills in this compartment was observed in the field. Interventions inside the gully are indicated, such as the construction of the impoundment, which is being dismantled by linear erosion, and the infilling with technogenic deposits, mainly in channel 3.

The geomorphological mapping presented in this study, in addition to analyzing the erosion dynamics of the gully, contributes to the methodological discussion on mapping with high-resolution images (HRI). This contribution occurs in two aspects: the proposal of a general compartmentalization of the erosion feature and the recording of individualized features within and around these compartments, with the application and adaptation of traditional symbolologies of geomorphological cartography.

Authors' Contributions: Conception, W.T.M. and A.S.; Methodology, W.T.M., A.S., J.A.C.P., S.L.A.; Investigation, W.T.M., A.S., J.A.C.P., S.L.A., and V.J.S.; Data processing and analysis, W.T.M., A.S., J.A.C.P., and S.L.A.; Writing – Initial version; W.T.M.; Writing – review and editing, A.S., J.A.C.P., S.L.A., and V.J.S. All authors read and agreed with the published version of the manuscript.

Data Availability: The raster files responsible for generating the morphometric maps and the vector files of the geomorphological map are available at <http://doi.org/10.5281/zenodo.15724795>.

Acknowledgements: The authors are grateful for the granting of a scholarship under Notice No. 06/2022 PIBIC/CNPq/UFU.

Conflict of Interest: The authors declare no conflict of interest.

7. References

1. AB'SÁBER, A. N. **Os domínios de natureza no Brasil: potencialidades paisagísticas**. São Paulo: Ateliê Editorial, 2003. 159. p.
2. ALBUQUERQUE, J. A.; ALMEIDA, J. A.; GATINONI, L. C.; ROVEDDER, A. P.; COSTA, F. S. Fragilidade de solos: uma análise conceitual, ocorrência e importância para o Brasil. In: CASTRO, S. S.; HERNANI, L. C. **Solos Frágeis: Caracterização, manejo e sustentabilidade**. 1ª Ed. Brasília: Embrapa, 2015. p. 25-50.
3. ALMEIDA FILHO, G. S.; TEIXEIRA FILHO, J. A importância da diferenciação dos processos erosivos lineares dos tipos ravina e boçoroca. In: XII Simpósio de Recursos Hídricos do Nordeste, 12., 2014, Natal – RN. **Anais...** Natal – RN: ABRH, 2014. ISSN 2359 – 1900.
4. ARANTES, A. E. Suscetibilidade à Erosão Laminar e Linear da Bacia Hidrográfica do Rio Vermelho e sua Relação com o Uso e Cobertura da Terra em 2012. **Revista Brasileira de Geografia Física**, v. 15, n. 6, p. 3032 – 3046, 2022. DOI: DOI: 10.26848/rbgf.v15.n.6.p3032-3046

5. ARAUJO, T. P. de. **Estudo do desencadeamento das erosões lineares concentradas em uma área do município de São Pedro/SP**. Dissertação (Mestrado em Geotecnia) - Escola de Engenharia de São Carlos, Universidade de São Paulo, São Carlos, 2011. DOI: <https://doi.org/10.11606/D.18.2011.tde-06122011-104236>
6. AUGUSTIN, D. H. R. R.; ARANHA, P. R. A. A ocorrência de voçorocas em Gouveira, MG: Características e Processos Associados. **Geonomos**. n. 14, p. 75-86, 2006. DOI: 10.18285/geonomos.v14i2.112
7. BARBOSA, M. I. M.; SILVEIRA, A.; MORAES, L. C.; ARAUJO, L. M. B. Expressão Geomorfológica Derivada de Diques Toleíticos na Região de Abadia dos Dourados (MG). In: 49º Congresso Brasileiro de Geologia, 49. 2018, Rio de Janeiro (RJ). **Anais...** Rio de Janeiro: Congresso Brasileiro de Geologia, 2018.
8. CARDOSO, R. Voçorocas voltam a engolir casas e amedrontar moradores em Buriticupu, no MA. **Portal G1**, Maranhão, 15 abril 2024. Available at: <<https://g1.globo.com/ma/maranhao/noticia/2024/04/15/vocorocas-voltam-a-engolir-casas-e-amedrontar-moradores-em-buriticupu-no-maranhao-video.ghtml>>. Accessed: 09 July 2024.
9. CASAGRANDE, D. **Mapa de suscetibilidade à erosão dos solos dos municípios consorciados à RIDES no Alto Paranaíba**. Trabalho de Conclusão de Curso (Graduação em Geologia) – Universidade Federal de Uberlândia, Monte Carmelo, 2023.
10. CASTRO, S.S; HERNANI, L.C. **Solos Frágeis: caracterização, manejo e sustentabilidade**. Brasília, DF : Embrapa, 2015. 367p.
11. CODEMIG. **Mapa Geológico Folha Estrela do Sul – SE.23-Y-A-IV**. CODEMIG, 2017. Escala 1: 100.000.
12. EMBRAPA. **Sistema brasileiro de classificação de solos**. 5ª Ed. – Brasília, DF: Embrapa, 2018. 356p.
13. ESTRADA, M. J. T. **Caracterização geológica-geotécnica do sítio urbano de Monte Carmelo e entorno – MG**. Trabalho de Conclusão de Curso (Graduação em Geologia) – Universidade Federal de Uberlândia, Monte Carmelo, 2023.
14. FIGUEIREDO, E.; FIGUEIREDO, S. **Planos de Voo Semiautônomos para Fotogrametria com Aeronaves Remotamente Pilotadas de Classe 3**. Rio Branco/AC: Embrapa - Circular Técnica, 2018. 56p. Available at:<<https://www.infoteca.cnptia.embrapa.br/infoteca/bitstream/doc/1100860/1/26750.pdf>>. Accessed: 30 May 2023.
15. FRANÇA JUNIOR, P; PELOGGIA, A.U.G. Os conceitos de antropoceno e tecnógeno e o estudo da humanidade como agente geomorfológico. In: FRAÇA JUNIOR, P. (Org.) **Geomorfologia do tecnógeno e antropoceno: perspectivas teóricas e estudos aplicados em ambientes urbanos**. Ituiutaba: Barlavento, 2020. p. 16 - 35.
16. FRÓES, R. Entenda o que são as voçorocas que formam crateras e abismos de terra no Maranhão. **Portal G1**, Maranhão, 02 mai. 2023. Available at: <https://g1.globo.com/ma/maranhao/noticia/2023/05/02/entenda-o-que-sao-as-vocorocas-fenomeno-que-provoca-abismos-de-terra-e-ameaca-engolir-cidade-no-maranhao.html>>. Accessed: 15 May 2023.
17. FOURNIER, F. **Climat et erosion**. Presses Universitaires de France, 1960.
18. GOOGLE. **GOOGLE EARTH**. 2023.
19. GOUDIE, A. **Encyclopedias of Geomorphology I**. Oxford: Routledge, 2004. 1156p.
20. GUERRA, A. J. T.; JORGE, M. C. O. Erosão dos solos e movimentos de massa-recuperação de áreas degradadas com técnicas de bioengenharia e prevenção de acidentes In: GUERRA, A. J. T.; JORGE, M. C. O. **Processos erosivos e recuperação de áreas degradadas**. São Paulo: Editora Oficina de Textos, 2017. p. 7-30.
21. GUERRA, A. J. T. O início do processo erosivo. In: GUERRA, A. J. T.; SILVA, A. S.; BOTELHO, R. G. M. **Erosão e Conservação dos solos: Conceitos, Temas e Aplicações**. 6ª Ed. Rio de Janeiro: Bertrand Brasil, 2010. p. 17-55.
22. GUERRA, A. J. T. Processos erosivos nas encostas. In: GUERRA, A. J. T.; CUNHA, S. B. **Geomorfologia uma atualização de bases e conceitos**. 10ª Ed. Rio de Janeiro: Bertrand Brasil, 2011. p. 149-209.
23. GUERRA, A. J. T. Técnicas e métodos utilizados no monitoramento dos processos erosivos. **Sociedade & Natureza**, v. 8, n. 15, p. 15-19, 1996. DOI: 10.14393/SN-v8-1996-61708.
24. HERNANI, L. C. FREITAS, P. L.; PRUSKI, F. F.; DE MARIA, I. C.; CASTRO FILHO, C.; LANDERS, J. N. Erosão e seu Impacto In: MANZATTO, C. V.; FREITAS JUNIOR, E.; PERES, J. R. R. **Uso Agrícola dos Solos Brasileiros**. Rio de Janeiro: Embrapa Solos, 2002. p. 46-60.
25. IBGE. **Malha Municipal**. Available at: <<https://www.ibge.gov.br/geociencias/organizacao-do-territorio/malhas-territoriais/15774-malhas.html>> Accessed: 30 March 2024.
26. IBGE. **Manual Técnico de Geomorfologia**. 2ª Ed. Rio de Janeiro: IBGE, 2009. 182p.
27. JULIAN, C.; NUNES, J. O. R. Uso de vant e geoprocessamento para cálculo de solo erodido em voçoroca localizada no distrito de Amadeu Amaral. Marília/SP - Brasil. **Revista Brasileira de Geomorfologia**, v. 21, n. 4, p. 835-845, 2020. DOI: 10.20502/rbg.v21i4.1818.
28. MOTTA, P.E.; BARUQUI, A.M.; SANTOS, H.G. **Levantamento de reconhecimento de média intensidade dos solos da região do Alto Paranaíba, Minas Gerais**. 1ª Ed. Rio de Janeiro: Embrapa Solos, 2004, 238 p.
29. MOURA, N. V.; SILVA, T. M.; GOUVEIA, I. C. M. C.; PEIXOTO, M. N. O.; FELIPPE, M. F.; OLIVEIRA, A. M. S.; PELOGGIA, A. U. G.; NOLASCO, M. C. Diretriz para mapeamento de formas de relevo tecnogênicas no Sistema Brasileiro de Classificação do Relevo. **Revista Brasileira de Geomorfologia**, v. 24, n. 4, 2023. DOI: 10.20502/rbgeomorfologia.v24i4.2466.

30. MOURA, R. V.; SANTOS, A. L. F.; ALVES JUNIOR, L. R. Mapeamento da Voçoroca em Anápolis-GO por Meio de Geotecnologias. **Brazilian Applied Science Review**, v. 5, n. 2, p. 1002-1012, 2021. DOI: 10.34115/basrv5n2-0.
31. NIR, D. **Man, a Geomorphological Agent: an introduction to anthropic geomorphology**. Jerusalém: Keter Publishing House, 1983. 175p.
32. NOVAIS, G. T. **Caracterização climática da mesorregião do Triângulo Mineiro/Alto Parnaíba e do entorno da Serra da Canastra (MG)**. Dissertação (Mestrado em Geografia) – Instituto de Geografia, Universidade Federal de Uberlândia (UFU), Uberlândia, 2011, 175 p.
33. OLIVEIRA, D. R.; CICERELLI, R. E.; ALMEIDA, T.; MAROTTA, G. S. Geração de Modelo Digital do Terreno a Partir de imagens obtidas por veículo aéreo não tripulado. **Revista Brasileira de Cartografia**, [S. l.], v. 69, n. 6, 2017. DOI: 10.14393/rbcv69n6-44316.
34. PEREIRA, J. S. O protagonismo da ciência geográfica nos estudos de erosão por voçorocamento. **Leia Cientista, Portal Comunica UFU**, 25 nov. 2020. Available at: < <https://antigo-comunica.ufu.br/noticia/2020/11/o-protagonismo-da-ciencia-geografica-nos-estudos-de-erosao-por-vocorocamento> > Accessed 14 August 2022.
35. PEREIRA, J. S.; RODRIGUES, S. C. Erosão por Voçorocas: Estado da Arte. In: CARVALHO JUNIOR, O. A.; GOMES, M. C. V.; GUIMARÃES, R. F.; GOMES, R. A. T. (Org). **Revisões de Literatura da Geomorfologia Brasileira**. Brasília: Universidade de Brasília, 2022. p. 499 – 525.
36. PIX4D. **Step 1: Before Starting a Project > 1. Designing the Acquisition Plan > a. Selecting the Image Acquisition Plan Type – PIX4Dmapper**. Available at: < <https://support.pix4d.com/hc/en-us/articles/202557459> >. Accessed: 15 October 2023.
37. RADEMANN, L. K.; TRENTIN, R. Novas geotecnologias aplicadas ao estudo geomorfológico: exemplo de morfometria da Voçoroca do Areal, Cacequi - RS. **Geotextos (Online)**, v. 16, p. 209-230, 2020. DOI: 10.9771/geo.v16i1.35474
38. RODRIGUES, S. C.; AUGUSTIN, C.H.R.R.; NAZAR, T. I. S. M. Mapeamento Geomorfológico do Estado de Minas Gerais: uma proposta com base na morfologia. **Revista Brasileira de Geomorfologia**, v. 24, n. 1, 2023. DOI: 10.20502/rbg.v24i1.2233
39. SILVA, B. F.; SILVEIRA, A.; BARBOSA, M. I. M. A cobertura natural e o uso da terra na bacia hidrográfica do Ribeirão do Brejo, Triângulo Mineiro: relações com os componentes do meio físico. **Revista Cerrados**, v. 21, n. 2, p. 348-376, 2023. DOI: 10.46551/rc24482692202331
40. SILVA, B. F.; SOUZA, G. F. LUPINACCI, C. M. Construção dos símbolos geomorfológicos para cartografia de detalhe em SIG. **Revista Brasileira de Geomorfologia**, v. 23, n. 4, 2022. DOI: 10.20502/rbg.v23i4.2201
41. SILVA, M. M.; LUPINACCI, C. M. Análise de variáveis morfométricas da Alta Bacia do Ribeirão da Boa Vista – Corumbataí (SP): subsídio ao planejamento ambiental de paisagem rural em escala de detalhe.. **Geografia**, Rio Claro – SP. v. 46, n. 1, 2021. ISSN: 1983-8700.
42. SILVEIRA, A.; CUNHA, C. M. L. Caracterização Geomorfológica em Área de Expansão Urbana: **Revista Brasileira de Geomorfologia**, v. 13, n. 3, p 235-244, 2012. DOI: 10.20502/rbg.v13i3.167
43. SIMON, A. H.; LUPINACCI, C. M. Introdução. In: SIMON, A.H.; LUPINACCI, C.M. (Org.). **A Cartografia Geomorfológica como Instrumento para o Planejamento**. Ed. UFPEL, Pelotas, v. 01, p. 08-11, 2019.
44. STABILE, R. A.; VIEIRA, B. C. Características morfológicas das feições erosivas da bacia Água da Faca, Piratininga (SP): considerações preliminares. In: VIII SIMPÓSIO NACIONAL DE GEOMORFOLOGIA, 8. 2010, Recife (PE). **Anais...** Recife (PE): [s.n.], 2010.
45. STEDANUTO, B. E.; LUPINACCI, C. M. The use of high resolution images in mapping of landscapes affected by erosion. **Agua y Territorio / Water and Landscape**, [S.I.], n. 23, e7291, 2023. DOI: 10.17561/at.23.7291.
46. TRICART, J. **Principes et Méthodes de la Geomorphologie**. Paris: Masson et cie, 1965.
47. VERSTAPPEN, H. T.; ZUIDAN, R. A. van. **ITC System of geomorphological survey**. Manual ITC Textbook, Netherlands: Enschede, v. 1, cap. 8, 1975.



This work is licensed under a Creative Commons Attribution 4.0 International License (<http://creativecommons.org/licenses/by/4.0/>) – CC BY. This license lets others distribute, remix, tweak, and build upon your work, even commercially, as long as they credit you for the original creation.